Effect of evaporation on step bunching induced by impurities

メタデータ	言語: eng
	出版者:
	公開日: 2018-06-29
	キーワード (Ja):
	キーワード (En):
	作成者:
	メールアドレス:
	所属:
URL	https://doi.org/10.24517/00051318

Effect of evaporation on step bunching induced by impurities

Masahide Sato

Information Media Center, Kanazawa University, Kakuma-machi, Kanazawa 920-1192, Japan

In this paper, we study the effect of the evaporation of adatoms and impurities on the step bunching induced by impurity. Keeping the ratio of the impingement rate of impurities F_{imp} to that of atoms F constant, we carry out Monte Carlo simulation. In the system with the evaporation of impurities, the growth rate of vicinal face R is proportional to F. This relation is the same as that without the evaporation of impurities. When F is small, the vicinal face is unstable. Compared with the system without the evaporation of impurities, the effect of impurities is weakened. In our simulation, step pairing occurs but large bunches are not formed. When we take account of the evaporation of both impurities and adatoms, the vicinal face grows when F is larger than the equilibrium value F_{eq}. R is not proportional to $(F - F_{eq})$ and large bunches are formed when F is small. In this paper, we also show how the impurity density on surface σ_{imp} and that incorporated in solid ρ_{imp} are related to the formation of step bunches.

I. INTRODUCTION

It has been well known that the impurities attaching to a vicinal face cause step bunching [1]. There are many theoretical studies and simulations for the step bunching induced by impurities [2–12]. For example, the time evolution of bunch size was studied by using one-dimensional models [2,3], in which the dependence of step velocity on the terrace width was assumed empirically. Pairing of steps, the logarithmic growth of bunch size, the formation of equidistant array of tight bunches, and the chaotic motion of bunches were shown to comply with the form of step velocity. Recently, the step bunching induced by impurities was also studied by two-dimensional models [4,6–12].

In experiments [13,14], it was pointed out that the mass transport processes of both impurity and growth unit are important for the incorporation of impurities in crystal in the case of a large growth unit such as a protein. The diffusion field of building blocks was not taken into account sufficiently in previous theoretical studies [1–12]. Crystals grew from solution in the experiments [13,14], and it was shown that mobile molecules in solution gradually become immobile on a crystal surface during incorporation into a solid [15]. This may be caused by the effect of the surface diffusion field: mobile molecules migrate on crystal surface more slowly than in solution and are immobilized after finding stable sites. Since the surface diffusion process may be important even in the case of growth from solution, we considered vapor growth and studied the effect of the surface diffusion field of adatoms on the step bunching induced by immobile impurities [16,17]. For the materials such as proteins, it is difficult to prepare specimens of high purity. Even in the case of the specimen of 99.99% purity, impurities affect the growth velocity and the morphology of crystal [18]. It is natural to consider that impurities are supplied on the surface with a constant rate during growth when the impurities are included in ingredients and supplied from a large vapor phase to a surface, and there are many theoretical studies, in which the supersaturation is fixed and the concentration of impurity is controlled. Thus, keeping the ratio of the impingement rate of impurities F_{imp} to that of atoms F constant, we carried out Monte Carlo simulation [17]. In the simulation, step bunching is induced by impurity. The tight step bunches formed by the same number of steps appear equidistantly when F is smaller than a critical value F_c. The rate-determining process affects the dependence of F_c on the terrace width l but does not change the process of the formation of tight bunches. The bunch size N_B, which is the number of steps in a bunch, increases with decreasing F. The density of impurities incorporated in solid, ρ_{imp}, is independent of the formation of step bunches, but the impurity density on surface σ_{imp} increases with increasing N_B.

We neglected the evaporation of both adatoms and impurities in our previous paper [17], which is one of the simplest cases, but their evaporation probably affects step behaviors during the step bunching induced by impurities. In this paper, taking the evaporation into account, we study the step bunching induced by impurities. Keeping the ratio of F_{imp} to F constant, we carry out Monte Carlo simulations. In Sec. II, we show our simple lattice model. In Sec. III, we show our results. In our Monte Carlo simulations, we study the step bunching in two cases: in one case it is only impurities that evaporate, and in the other case both impurities and adatoms evaporate. For each case, we show how σ_{imp} and ρ_{imp} are affected by the formation of step bunches. In Sec. IV, we summarize our results.

II. MODEL

We modify the model used in Ref. [17] for Monte Carlo simulations. We consider a vicinal face with a square lattice (Fig. 1). The lattice constant a is the unity and the system size is given by $L_x \times L_y$. On the vicinal face, n_s steps are parallel to the x axis on average and advance in the y direction. Since
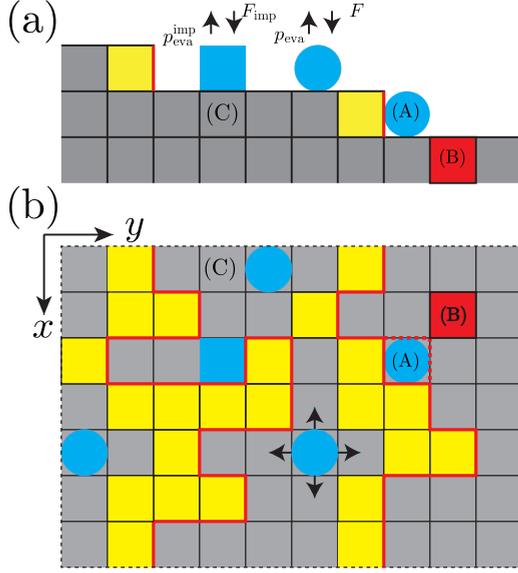
FIG. 1. (a) Side view and (b) top view of a vicinal face formed by a square lattice. Blue (dark) circles and blue (dark) squares represent adatoms and impurities on surface, respectively. Red (thick) lines are steps. Yellow (bright) squares are step atoms, which are the solid atom forming steps. Adatom (A) represents an adatom attaching to step atoms and impurity (B) represents an impurity incorporated in solid.

we forbid two-dimensional nucleation on terraces, the number of steps is kept constant.

We use a periodic boundary condition in the x direction and a helical boundary condition in the y direction. Initially, the steps are straight and equidistant. Adatoms are located on lattice sites randomly and there are no impurities on the surface.

In our simulation, we distinguish adatoms, impurities, solid atoms, and impurities incorporated in solid [16,17]. The elementary processes we take into account are the migration of adatoms, the evaporation of both adatoms and impurities, and the solidification of the adatoms attaching to steps. We also take account of melting of the step atoms, which are solid atoms forming steps. In a Monte Carlo trial, we choose an adatom, an impurity, or a step atom. When we select an adatom, we try the evaporation of the adatom with probability p_{eva}. When the adatom does not evaporate in that trial, we subsequently try to move it to one of the neighboring sites as a diffusion trial: we choose one of the neighboring sites randomly and move the adatom to the chosen site if it is not occupied by either an adatom or impurity. Since we neglect the Ehrlich-Schwoebel effect [19,20], the adatom can migrate between the upper and lower terraces over a step edge. To set the diffusion coefficient D_{s} to unity, the time increase during a diffusion trial is given by $1/4N$, where N is the number of adatoms on the surface. p_{eva} is related to the lifetime of adatoms τ as $p_{\mathrm{eva}} = 1/4\tau$.

When an adatom attaches to step atoms after a diffusion trial as with adatom (A) in Fig. 1, we try the solidification of this adatom. If the adatom is not solidified, the adatom stays on the site until the adatom is chosen for another diffusion trial again. The solidification probability p_{s}, which is determined by both increment of the step energy ΔE_{s} and chemical potential gain

per atom ϕ, is given by [21]

$$p_{\mathrm{s}} = \left[1 + \exp\left(\frac{\Delta E_{\mathrm{s}} - \phi}{k_{\mathrm{B}}T} \right) \right]^{-1}, \qquad (1)$$

where k_{B} is the Boltzmann constant and T is temperature. When the number of the step atoms contiguous to the adatom is n_{n}, ΔE is given by $2\epsilon(2 - n_{\mathrm{n}})$, where ϵ is the step energy per step length.

When a step atom is selected in a trial, we check whether either adatom or impurity is present on the top of the selected step atom. If there is an adatom or impurity on the top of the selected step atom, melting of the step atom is not allowed. If the top of the selected step atom is empty, we try a melting trial of the selected step atom. When the step atom is not melted, it stays there as a step atom. When the step atom is melted, the step atom changes into an adatom. It stays on the site until it is selected for a diffusion trial. If solid atoms incorporated in a completed layer are contiguous to the melted step atom, the neighboring solid atoms change into step atoms. They may be chosen and melted in another melting trial. The melting probability p_{m} is given by [21]

$$p_{\mathrm{m}} = \left[1 + \exp\left(\frac{\Delta E_{\mathrm{s}} + \phi}{k_{\mathrm{B}}T} \right) \right]^{-1}. \qquad (2)$$

In equilibrium, the solidification frequency is equal to the melting frequency at kink sites. When the adatom density is small, the equilibrium adatom density c_{eq}^0 satisfies $p_{\mathrm{s}}c_{\mathrm{eq}}^0 = p_{\mathrm{m}}(1 - c_{\mathrm{eq}}^0)$ at the kink sites. Since $\Delta E_{\mathrm{s}} = 0$ at the kink sites, the equilibrium adatom density c_{eq}^0 is given by [21]

$$c_{\mathrm{eq}}^0 = \left[1 + \exp\left(\frac{\phi}{k_{\mathrm{B}}T} \right) \right]^{-1}. \qquad (3)$$

Owing to the solidification of adatom attaching to step atoms, which are the solid atoms forming steps, and melting of step atoms, the step form changes and fluctuates. When $\epsilon/k_{\mathrm{B}}T$ is large, step fluctuations are small enough to neglect overhangs of steps. The step stiffness $\tilde{\beta}$ is given by [21]

$$\tilde{\beta} = \frac{2k_{\mathrm{B}}T}{a} \sinh^2 \frac{\epsilon}{2k_{\mathrm{B}}T}. \qquad (4)$$

When we select an impurity, we try its evaporation. The evaporation probability $p_{\mathrm{eva}}^{\mathrm{imp}}$ is given by $p_{\mathrm{eva}}^{\mathrm{imp}} = 1/4\tau_{\mathrm{imp}}$, where τ_{imp} is the lifetime of impurity. In our simulation, we neglect the difference in bonding energy in the vertical direction between impurity and adatom. In the horizontal direction, we neglect the bonding between an impurity and solid atoms and that between an impurity and impurities incorporated in solid. The impurity, which is not incorporated in solid, does not interact with adatoms, step atoms, and impurities. However, when four neighboring sites around an impurity are occupied by either solid atoms or impurities as with impurity (B) in Fig. 1, we consider that the impurity is incorporated in solid phase. The impurity incorporated in solid is not distinguished from a solid atom. When the impurity incorporated in solid forms surface like impurity (B), another impurity and atom can impinge on it. An adatom can also migrate on the impurity, which is incorporated in a solid. When the adatom on the top of the impurity incorporated in a solid is solidified, the

impurity incorporated in solid phase is buried into crystal. On the contrary, when an impurity incorporated in a solid phase, which is buried into crystal, appears in the solid layer forming surface by melting the upper solid layers and one of the neighboring solid atoms of this impurity is melted, the impurity incorporated in the solid phase returns to an impurity, which is not incorporated in the solid phase. In our simulation, we also neglect the migration of impurities on surface. After some diffusion trials, we impinge both adatoms and impurities. We count the time interval from the last impingement trial, Δt, and calculate the numbers of impinged adatoms and impurities as $FL_xL_y\Delta t$ and $F_{imp}L_xL_y\Delta t$, where F and F_{imp} are the impingement rates of adatoms and impurities, respectively. We select a site for an adatom or impurity to impinge on. If an adatom or impurity that is not incorporated in a solid is not present on the selected site, the adatom or impurity impinge on the top of the site. If the site is occupied by an adatom or impurity that is not incorporated in a solid, the impingement of adatoms and that of impurities are not allowed. We continue to select another site and to try the impingement until all estimated numbers of adatoms and impurities impinge. In this paper, we consider a specimen such as a proteins in which impurities are not removed perfectly and remaining impurities affect the growth process even with a high purity [18]. In the system, the effect of impurities on the growth rate is remarkable when the supersaturation is low. When the impurities are included in ingredients and impinge from large environment to the surface, the ratio of impurity to atoms in the environment does not change during growth. It is probably natural that the impurities impinge with a constant rate. Thus, we keep F_{imp}/F constant. We change F and study step behaviors during the step bunching.

III. RESULTS OF SIMULATIONS

In our simulation, we consider two cases. In one case, we take account of the evaporation of impurities but neglect the evaporation of adatoms. In the other case, both adatoms and impurities evaporate. In the two cases, the system size and step number n_s are the same: the system size is $L_x \times L_y = 256 \times 256$ and n_s is 8. Since we set ϵ/k_BT to 2.0 and ϕ/k_BT to 3.0, c_{eq}^0 and $\tilde{\beta}/k_BT$ are estimated to be 4.724×10^{-2} and 2.76, respectively. Thus, the adatom density is small and there are many kinks on steps. F_{imp}/F is set to 4×10^{-3} and τ_{imp} is set to 10^5. Since $F < 10^{-4}$, the impurity density on surface, σ_{imp}, is not so large.

A. Case with the evaporation of impurities

First, we study step bunching in the case that it is only impurities that evaporate. Figure 2 shows the relation between the growth rate of crystal height R and the impingement rate F. Since the evaporation of adatoms is neglected and the step height is set to a, $R = F$ as in the case of our previous study [17]. Figure 3 shows snapshots of vicinal face. When $F = 9.0 \times 10^{-5}$ [Fig. 3(a)], the step bunching is not induced by impurities. The steps are straight and equidistant on average during growth. The vicinal face is unstable when $F = 6.0 \times 10^{-5}$ [Fig. 3(b)]. Fluctuations of the distance between steps are large, but tight bunches are not formed. When F decreases,
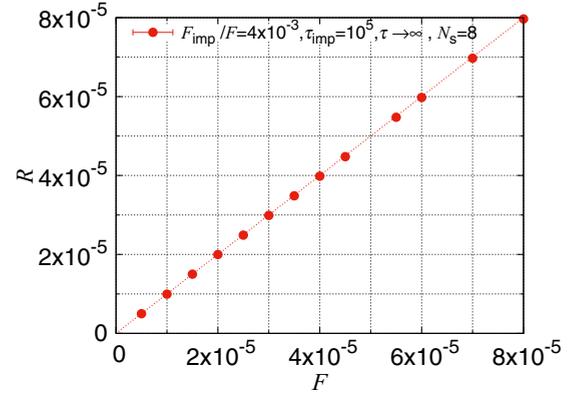
FIG. 2. Dependence of growth rate of crystal height R on the impingement rate of adatoms F. The data are averaged over ten individual runs.

the vicinal face becomes unstable. When $F = 4.0 \times 10^{-5}$ and 1.0×10^{-5} [Figs. 3(c) and 3(d)], tight step pairs are formed.

In our previous paper [17], we showed that the bunch size N_B, which is the number of steps in a bunch, increases with decreasing F if impurities do not evaporate. When the steps are equidistant with the step distance l, the velocity of the steps V_s is given by $V_s = aFl$. Since the time interval of step passage is given by l/V_s, the impurity density in front of the step, σ_{imp}^s, is given by F_{imp}/Fa. Thus, if the steps are equidistant and no impurity evaporates, σ_{imp}^s is constant. When the step distances are fluctuated, σ_{imp}^s of the step having a large front terrace becomes larger than that of other steps. When F is sufficiently large, the step overcomes the deceleration caused by impurities and the steps return to equidistant again. However, when F is small, the step cannot overcome the deceleration by impurity. The step velocity decreases and the step pairing occurs. Large bunches are formed by the similar scenario, but F needs to be smaller than that causing the step pairing. When the impurities evaporate, the deceleration caused by impurity is weakened. The steps can overcome the increase in the impurities, which is caused by large front terrace by the fluctuation of terrace width, more easily than that without the evaporation of impurity. The formation of large bunches becomes more difficult than that without the evaporation of impurity. With the parameters we used in our simulation, step pairing occurs but large bunches are not formed. When F approaches 0, F_{imp} also approaches 0. Thus, the effect of the evaporation of impurity becomes large and the tight step pairs are not formed.

We investigate how the average impurity density on surface, σ_{imp}, and the ratio of impurities incorporated in solid to the solidified atoms, ρ_{imp}, depend on F. Figure 4(a) shows the dependence of σ_{imp} on F. To clarify the effect of the formation of step pairs on σ_{imp}, we also carry out simulations in the system with one step. Since the system size $L_x \times L_y$ is 256×32 in the simulation, the terrace width is kept the same as that in the simulation with eight steps. When F is large, σ_{imp} in the system with eight steps is as large as that in the system with one step, which is because the vicinal face is stable as shown in Fig. 3(a). With decreasing F, σ_{imp} in the system with eight steps increases when $4 \times 10^{-5} < \sigma_{imp} < 8 \times 10^{-5}$ and decreases
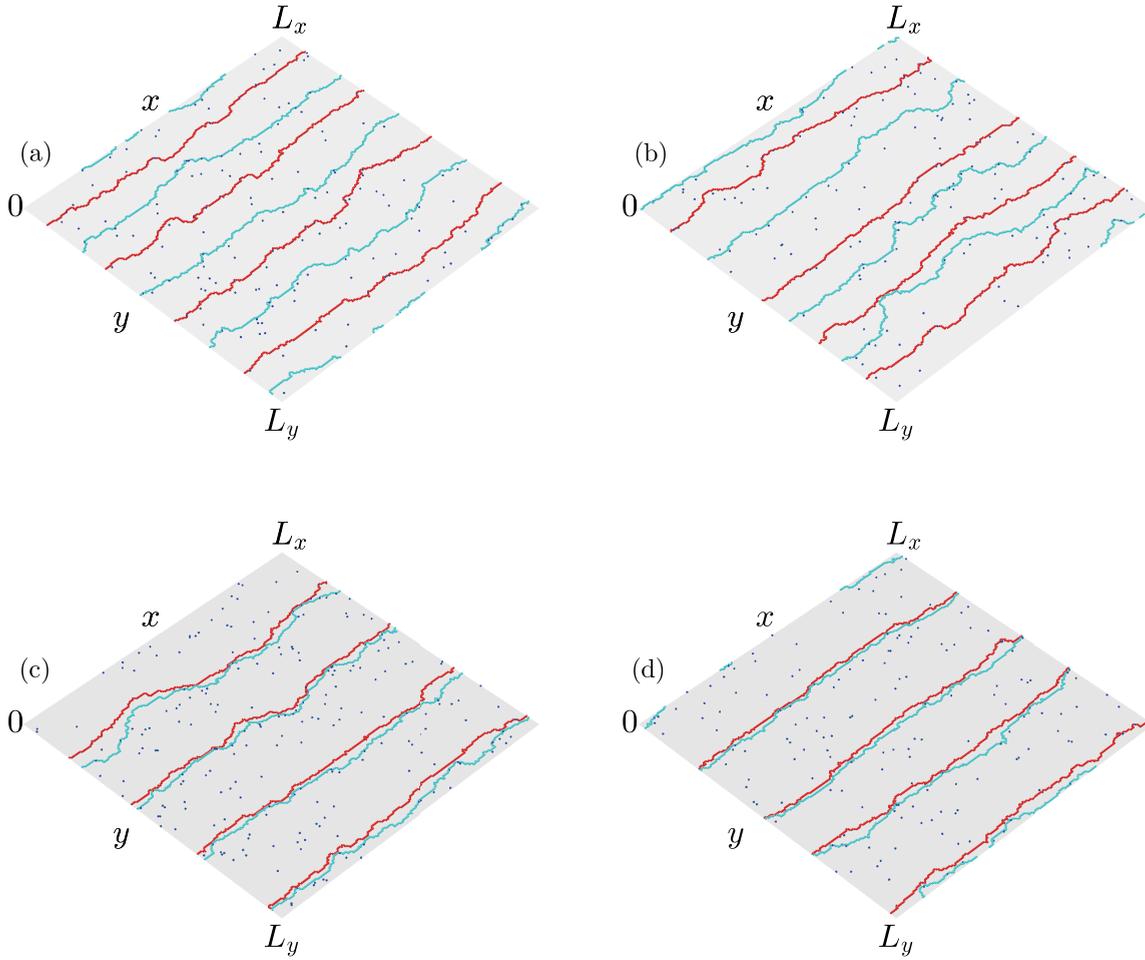
FIG. 3. Snapshots of vicinal face. F and time t are (a) $F = 9.0 \times 10^{-5}$ at $t = 2.4 \times 10^6$, (b) $F = 6.0 \times 10^{-5}$ at $t = 2.4 \times 10^6$, (c) $F = 4.0 \times 10^{-5}$ at $t = 3.2 \times 10^6$, and (d) $F = 1.0 \times 10^{-5}$ at $t = 3.5 \times 10^6$. To clarify the figures, we change the colors of steps alternatively. Dots on terraces represent impurities.

when $F < 4 \times 10^{-5}$. The decrease in σ_{imp} is different from the dependence of σ_{imp} on F in the system without the evaporation of impurities.

Figure 4(b) shows the dependence of ρ_{imp} on F. By using the number of impurities incorporated in solid, ΔN_{imp}, and that of solidified adatoms ΔN, we define ρ_{imp} as $\rho_{imp} = \Delta N_{imp}/\Delta N$.

When there is no evaporation of impurities, all the impinging impurities are incorporated in the solid phase and ρ_{imp} should be equal to F_{imp}/F. With the evaporation of impurities, ρ_{imp} decreases with decreasing F as shown in Fig. 4(b). In the system with eight steps, ρ_{imp} is a little smaller than that in the system with one step when step pairs are formed.
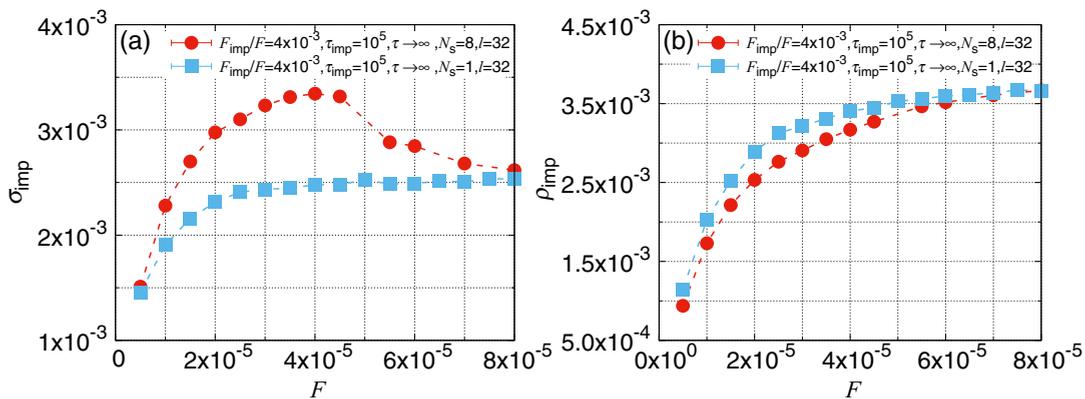
FIG. 4. Dependence of (a) the average adatom density on surface, σ_{imp}, on F and (b) the ratio of impurities incorporated in solid to solidified atoms, ρ_{imp}, on F. The data are averaged on ten individual runs.
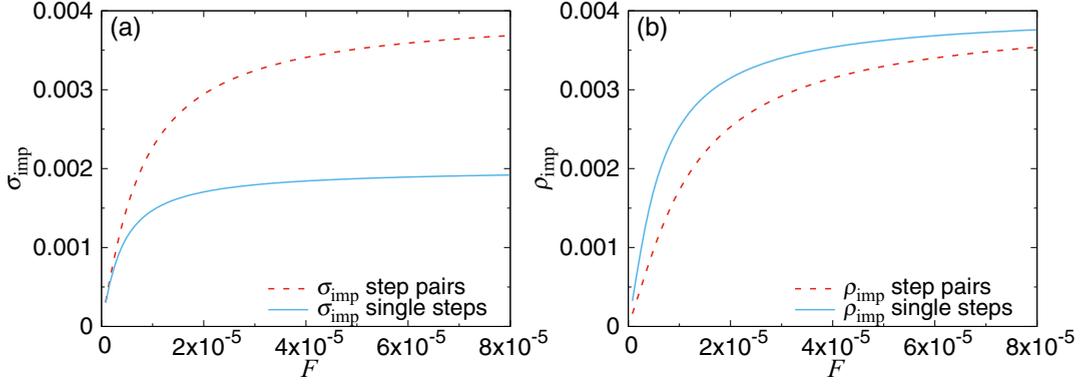
FIG. 5. Dependence of (a) σ_{imp} and (b) ρ_{imp} on F, where $\tau_{\text{imp}} = 10^5$, $\Omega = 1$, and $l = 32$.

Assuming that the steps are straight, we consider why both ρ_{imp} and σ_{imp} depend on F as shown in Figs. 4(a) and 4(b). When we neglect the surface diffusion of impurities, the time evolution of impurity density c_{imp} is given by

$$\frac{dc_{\text{imp}}}{dt} = F_{\text{imp}} - \frac{c_{\text{imp}}}{\tau_{\text{imp}}}. \tag{5}$$

The impurities attaching to the surface are incorporated in a solid when a step passes by. Immediately after the step passing by, there are no impurities attaching to the surface on the top of step atoms. The surface area cleaned by the step is polluted until the next step passes by. When the steps are equidistant with the step distance l and the step velocity is given by V_{s}, the time interval of step passage is given by l/V_{s}. Since ρ_{imp} is the same as the impurity density immediately in front of a step, σ_{imp} and ρ_{imp} are given by

$$\sigma_{\text{imp}} = \tau_{\text{imp}} F_{\text{imp}} \left\{ 1 + \frac{V_{\text{s}}\tau_{\text{imp}}}{l} \left[\exp\left(-\frac{l}{V_{\text{s}}\tau_{\text{imp}}} \right) - 1 \right] \right\}, \tag{6}$$

$$\rho_{\text{imp}} = \Omega \tau_{\text{imp}} F_{\text{imp}} \left[1 - \exp\left(-\frac{l}{V_{\text{s}}\tau_{\text{imp}}} \right) \right], \tag{7}$$

where $\Omega = a^2 = 1$ is the atomic area. When we assume that the tight step bunches whose size is N_{B} are formed equidistantly, the distance between the bunches is approximately given by $N_{\text{B}}l$. The impurity density in the tight bunches is negligibly small. When adatoms do not evaporate, V_{s} is not affected by impurity and given by $\Omega F l$ as shown in Fig. 2. When the step bunches are tight, we can treat the tight bunches as single steps whose height is N_{B}. Since the distance between the tight bunches whose size is N_{B} is given by $N_{\text{B}}l$, the velocity of the bunches is expressed as

$$V_{\text{B}} = \frac{\Omega F N_{\text{B}} l}{N_{\text{B}}} = V_{\text{s}}. \tag{8}$$

Since the velocity of the bunches V_{B} is independent of N_{B} and equal to V_{s}, the impurity densities σ_{imp} and ρ_{imp} are

expressed as

$$\sigma_{\text{imp}} = \tau_{\text{imp}} F_{\text{imp}} \left\{ 1 + \frac{V_{\text{s}}\tau_{\text{imp}}}{N_{\text{B}}l} \left[\exp\left(-\frac{N_{\text{B}}l}{V_{\text{s}}\tau_{\text{imp}}} \right) - 1 \right] \right\}, \tag{9}$$

$$\rho_{\text{imp}} = \frac{\Omega \tau_{\text{imp}} F_{\text{imp}}}{N_{\text{B}}} \left[1 - \exp\left(-\frac{N_{\text{B}}l}{V_{\text{s}}\tau_{\text{imp}}} \right) \right]. \tag{10}$$

Figure 5 shows the dependence of both ρ_{imp} and σ_{imp} on F. In our simulation, τ_{imp} and F_{imp}/F are set to 10^5 and 4×10^{-3}, respectively. $V_{\text{s}}\tau_{\text{imp}}/l$ is expressed as $\Omega F \tau_{\text{imp}} = 10^5 F$ and $\tau_{\text{imp}} F_{\text{imp}}$ is equal to $4 \times 10^2 F$. In a vicinal face with eight steps, ρ_{imp} becomes larger and σ_{imp} becomes smaller than those with one step when $F \approx 4 \times 10^{-5}$. Since step pairing occurs at $F \approx 4 \times 10^{-5}$ in Fig. 3(c), the increase in σ_{imp} and decrease in ρ_{imp} are caused by formation step pairs. The changes in σ_{imp} and ρ_{imp} qualitatively agree with Eqs. (9) and (10).

B. In case with the evaporation of both impurities and adatoms

Next, we study step bunching in the case that both impurities and adatoms evaporate. Since we set τ to 512, the surface diffusion length of adatoms, x_{s}, is given by $x_{\text{s}} = \sqrt{D_{\text{s}}\tau} = 22.6$. In our simulation, We set the step distance l to 32. Since l is smaller than twice x_{s}, the steps located equidistantly on the vicinal face interact via the surface diffusion field. When tight step pairs are formed equidistantly, the distance between the step pairs is longer than x_{s}. Thus, the step pairs hardly interact via the surface diffusion field. When the adatoms evaporate, the steps are not expected to advance when F is smaller than $F_{\text{eq}} = c_{\text{eq}}/\tau = 9.22 \times 10^{-5}$ in the system without impurities.

Figure 6 shows the dependence of R on F. The step kinetic coefficient K is estimated to about 2 [17,21], so that K satisfies $Kx_{\text{s}}/D_{\text{s}} > 1$. If we neglect the effect of impurities, R is expected to be proportional to $(F - F_{\text{eq}})$ from the one-dimensional step flow model [22]. Since K is large but finite [17,21], the inclination of R expected from a step flow model is slightly smaller than 1. When $F > 2.2 \times 10^{-4}$, R with eight steps agrees with the velocity expected by the step flow model. When $1.3 \times 10^{-4} < F < 2.2 \times 10^{-4}$, however, R is smaller than the expected value, which is similar to the growth velocity in Refs. [18,23]. The slow growth is probably caused by step bunching because the slow growth in this F region is not observed in the system with one step. Since F_{imp}/F is kept constant in our simulation, the ratio of F_{imp}
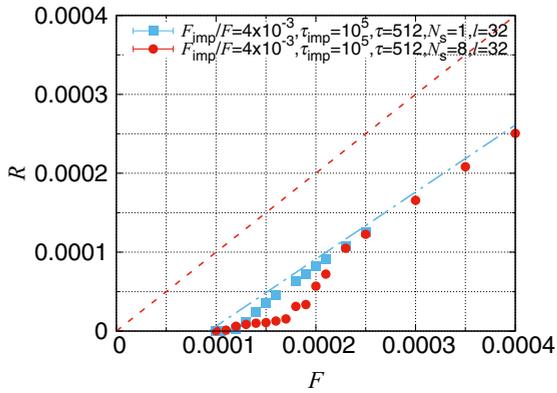
FIG. 6. Dependence of R on F. Dot-dashed line represents R expected from the one-dimensional step flow model, where effects of impurities are neglected. Dashed line represents $R = F$. The data are averaged over ten individual runs.

to the supersaturation, which is proportional to $(F - F_{eq})$, increases near F_{eq}. Thus, although F is larger than that in the case without the evaporation of adatoms, the step bunching is caused easily by the small fluctuation of step distance.

When the bunches whose size $N_B \geqslant 2$ are formed equidistantly by the step bunching, the distance between the bunches is larger than x_s. Roughly speaking, the bunches can catch the adatom in x_s from both sides of terraces. Thus, the number of adatoms caught by a bunch is independent of N_B if the bunches are equidistant. Since the adatoms caught by each bunch are expended by the advancing N_B steps in a bunch, the velocity of a bunch decreases with increasing N_B and the step bunches move slowly. When $F_{eq} \leqslant F \leqslant 1.3 \times 10^{-4}$, R is very small and hardly differs in the two systems. This slow growth is probably caused by step pinning by impurity [1]. The pinned step cannot move if thermal fluctuation is neglected. However, the impurity size is the same as the solid atom size in our simulation. The steps surround impurities and incorporate the impurities into a completed solid layer, so that the steps can advance slowly by thermal fluctuation.

Figure 7 shows snapshots of steps on the vicinal face with eight steps. When $F = 2.5 \times 10^{-4}$ [Fig. 7(a)], the steps are fluctuated but the step bunching is not caused by impurity. When $F = 2.1 \times 10^{-4}$ [Fig. 7(b)], the vicinal face is unstable and step pairs are formed but large bunches are not formed. When $F = 1.5 \times 10^{-4}$ [Fig. 7(c)], all the steps gather and a large straight step bunch is formed. Figures 7(b) and 7(c) agree with our expectation from Fig. 6: the difference of R from the
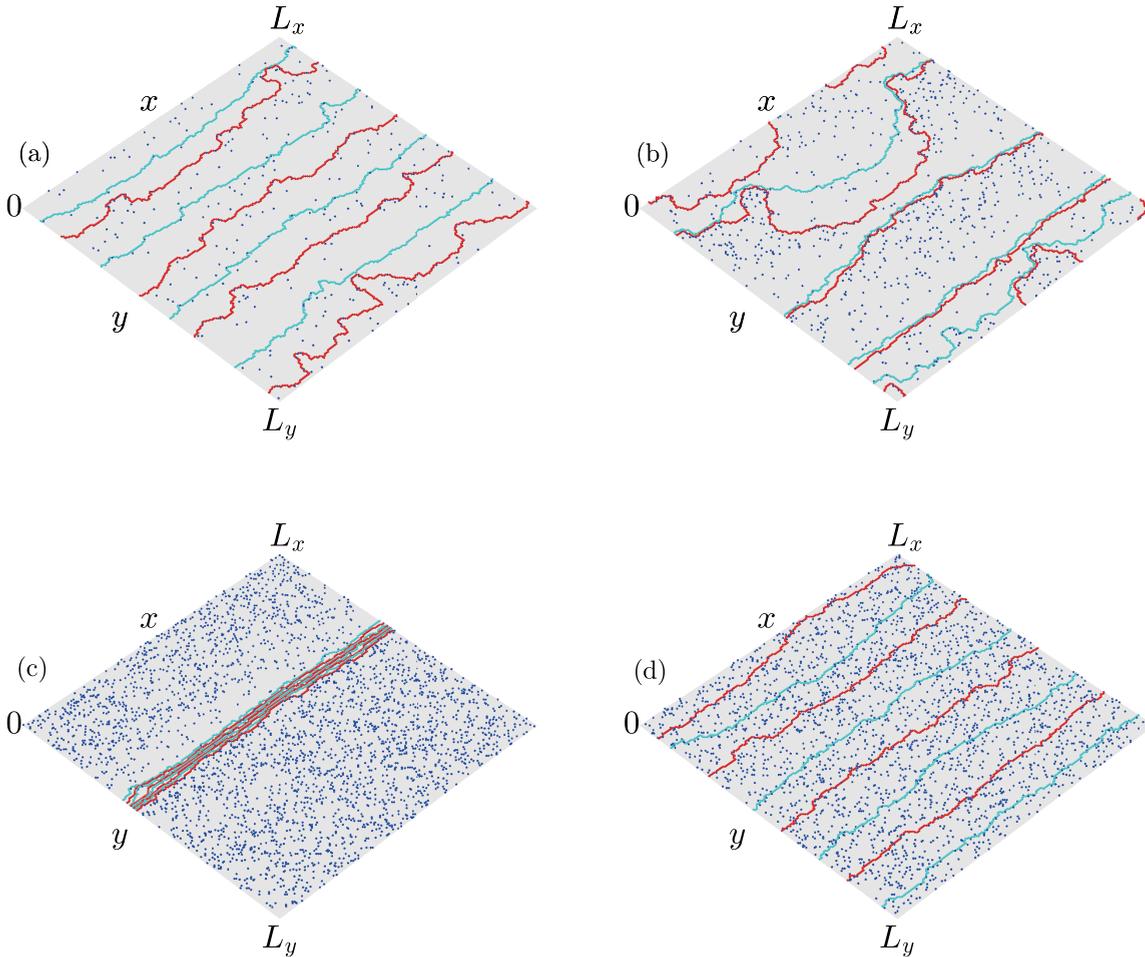
FIG. 7. Snapshots of vicinal face with the evaporation of adatoms. F and t are (a) 2.5×10^{-4} and 5.8×10^5, (b) 2.1×10^{-4} and 1.3×10^6, (c) 1.5×10^{-4} and 4.3×10^6, and (d) 1.0×10^{-4} and 5.1×10^6, respectively. To clarify the figures, we change the step colors alternatively. Dots on terraces represent impurities.
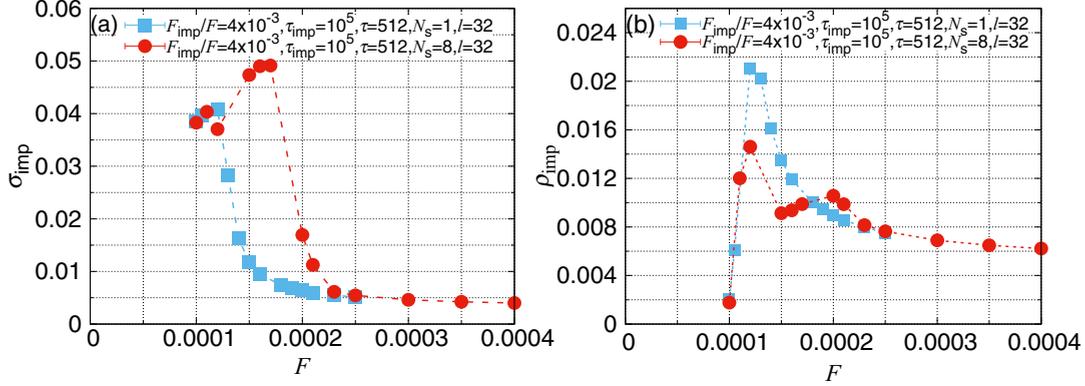
FIG. 8. Dependence of (a) σ_{imp} and (b) ρ_{imp} on F. The data are averaged over ten individual runs.

expected value is caused by the formation of step bunches. N_{B} decreases when F approaches F_{eq}, and the step bunching is not observed even in a long simulation when F is very close to F_{eq} [Fig. 7(d)].

We study how σ_{imp} and ρ_{imp} are affected by the formation of step bunches. Figure 8(a) shows the dependence of σ_{imp} on F. In the system with one step, σ_{imp} increases with decreasing F and approaches 0.04 when F approaches F_{eq}. The steps stop and the impurities are not incorporated in solid when F is equal to F_{eq}, so we expect that σ_{imp} approaches $F_{\mathrm{imp}}/\tau_{\mathrm{imp}}$ when F becomes close to F_{eq}. Since F_{imp}/F is 4.0×10^{-3} and τ_{imp} is set to 10^{-5} in our simulation, $F_{\mathrm{imp}}/\tau_{\mathrm{imp}}$ is estimated to 0.04 when $F = 10^{-4}$. Thus, σ_{imp} near F_{eq} in Fig. 8(a) agrees with the expectation.

The dependence of σ_{imp} on F in the system with eight steps is different from that in the system with one step. With decreasing F, σ_{imp} increases faster than that in the system with one step and becomes much larger than 0.04. Figure 8(b) shows the dependence of ρ_{imp} on F. In the system with one step, ρ_{imp} has one peak near F_{eq}. When $N_{\mathrm{s}} = 8$, the dependence of ρ_{imp} on F is more complicated that in the system with one step: two maxima appear when $F = 2.0 \times 10^{-4}$ and 1.2×10^{-4}. Since ρ_{imp} decreases with decreasing F monotonically in Fig. 4(b), the evaporation of adatoms makes the dependence of ρ_{imp} on F more complicated.

In the case with the evaporation of both adatoms and impurities, σ_{imp} and ρ_{imp} are different from those in the case that it is only impurities that evaporate. The differences in σ_{imp} and ρ_{imp} between the two cases are caused by the form of the velocity of bunches. Since straight tight bunches are formed in Fig. 7(c), we assume that tight bunches are located equidistantly. For simplicity, we regard the kinetic coefficient as infinitely large. When the bunches are tight and the distance between the bunches is given by L, the bunches are regarded as the single step whose velocity is given by

$$V_{\mathrm{s}} = 2\Omega \frac{D_{\mathrm{s}}\tau}{x_{\mathrm{s}}}(F - F_{\mathrm{eq}})\tanh\left(\frac{L}{2x_{\mathrm{s}}}\right). \quad (11)$$

When we neglect the impurities, V_{B} is related to V_{s} as $V_{\mathrm{B}} = V_{\mathrm{s}}/N_{\mathrm{B}}$ and expressed as

$$V_{\mathrm{B}} = 2\Omega \frac{D_{\mathrm{s}}\tau}{N_{\mathrm{B}}x_{\mathrm{s}}}(F - F_{\mathrm{eq}})\tanh\left(\frac{L}{2x_{\mathrm{s}}}\right), \quad (12)$$

where L is the distance between bunches. When the bunch size is N_{B}, L is given by $N_{\mathrm{B}}l$. Since L is larger than the surface diffusion field in our simulation, V_{B} is approximated as $V_{\mathrm{B}} = \Omega(F - F_{\mathrm{eq}})x_{\mathrm{s}}/N_{\mathrm{B}}$. Thus, σ_{imp} and ρ_{imp} are given by

$$\sigma_{\mathrm{imp}} = \tau_{\mathrm{imp}}F_{\mathrm{imp}}\left\{1 + \frac{\Omega x_{\mathrm{s}}(F - F_{\mathrm{eq}})\tau_{\mathrm{imp}}}{N_{\mathrm{B}}^2 l}\right.$$
$$\left. \times \left[\exp\left(-\frac{N_{\mathrm{B}}^2 l}{\Omega x_{\mathrm{s}}(F - F_{\mathrm{eq}})\tau_{\mathrm{imp}}}\right) - 1\right]\right\}, \quad (13)$$

$$\rho_{\mathrm{imp}} = \frac{\Omega \tau_{\mathrm{imp}} F_{\mathrm{imp}}}{N_{\mathrm{B}}}\left[1 - \exp\left(-\frac{N_{\mathrm{B}}^2 l}{\Omega x_{\mathrm{s}}(F - F_{\mathrm{eq}})\tau_{\mathrm{imp}}}\right)\right]. \quad (14)$$

Figure 9 shows σ_{imp} and ρ_{imp} given by Eqs. (13) and (14), where $N_{\mathrm{B}} = 1, 2, 4$, and 8. When F approaches F_{eq}, σ_{imp} converges to 0.04 from the lower side in the cases of $N_{\mathrm{B}} = 1$ and 2. When $N_{\mathrm{B}} = 4$ and 8, σ_{imp} approaches 0.04 from the upper side [Fig. 9(a)]. When we take account of the formation of large bunches with small F and the decrease in N_{B} near $F = F_{\mathrm{eq}}$, σ_{imp} in Fig. 9(a) qualitatively agrees with Fig. 8(a).

In Fig. 9(b), ρ_{imp} increases with increasing N_{B} when F is large. On the contrary, ρ_{imp} decreases with increasing N_{B} and ρ_{imp} with single steps is larger than that with bunches when F is near F_{eq}. In our simulation, N_{B} increases with decreasing F when F is small, but N_{B} decreases and finally the step bunches are not formed when F becomes very close to F_{eq}. When we take account of the dependence of N_{B} on F, we can understand the formation of two peaks qualitatively: the peak at large F is caused by the formation of large bunches and the peak at small F is induced by the decrease in N_{B} with decreasing F.

IV. SUMMARY

In this paper, we studied the effect of the evaporation of both adatoms and impurities on the step bunching induced by impurity. Keeping F_{imp} to F constant, we carried out Monte Carlo simulation. When neither impurities nor adatoms evaporate [17], the step bunching occurs when F is small. The bunch size N_{B} increases with decreasing F. When the evaporation of impurities is added, the effect of impurities causing the step bunching is weakened. Step
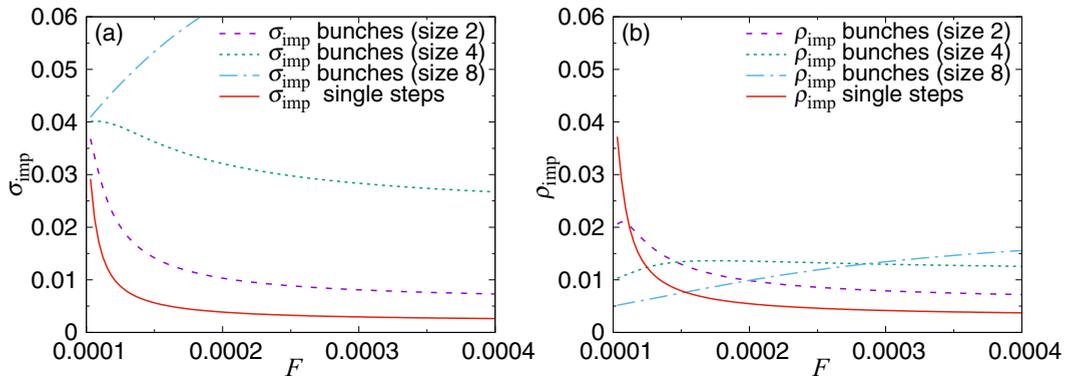
FIG. 9. Dependence of (a) σ_{imp} and (b) ρ_{imp} on F. We use $F_{\mathrm{eq}} = 10^{-4}$, $x_{\mathrm{s}} = 16\sqrt{2}$, $\tau_{\mathrm{imp}} = 10^5$, $\Omega = 1$, and $l = 32$.

pairs were formed but large bunches did not appear in our simulation.

We also carried out simulation taking account of the evaporation of both adatoms and impurities. The vicinal face does not grow when F is smaller than F_{eq}. If we neglect the impurities, R is expected to be proportional to $(F - F_{\mathrm{eq}})$. When F is near F_{eq}, however, R is much slower than the expected value. The slow growth is caused by the step pinning induced by impurity. The step does not advance in the system with a lot of impurities when the effect of thermal noise is not taken into account, but the step incorporates impurities when the step surrounds the impurity by thermal fluctuation. In addition, step pinning is weakened since the impurities evaporate in our simulation. Thus, the step can advance with slow velocity.

When F goes a little far away from F_{eq}, the growth velocity increases but is still smaller than the expected value, which is similar to Refs. [18,23]. The slow growth in the F region is probably caused by step bunching. Large bunches are not formed when the evaporation of adatoms are neglected, but the formation of large bunches occurs when both adatoms and impurities evaporate. Since we kept F_{imp} to F constant in our simulation, the ratio of F_{imp} to $F - F_{\mathrm{eq}}$ becomes large when F approaches F_{eq}. The increase in the ratio of F_{imp} to $F - F_{\mathrm{eq}}$ by decreasing F acts in the same way that the increase in the ratio

by the increase in F_{imp}, which probably causes the formation of large bunches. When F sufficiently goes far away from F_{eq}, R increases sharply with increasing F and approaches the expected value.

When we take account of the evaporation of impurities but neglect the evaporation of adatoms, ρ_{imp} decreases with decreasing F and σ_{imp} becomes large in small F region owing to the formation of step pairs. The behaviors of both σ_{imp} and ρ_{imp} are different when both adatoms and impurities evaporated: σ_{imp} becomes large and ρ_{imp} has two peaks in the F region where the step bunching occurs. The difference is caused by the form of V_{B}. In our simulation, we neglected the surface migration of impurities. When we take account of the migration in our model, the tightness of step bunches and the dependence of both σ_{imp} and ρ_{imp} on F may change. Now, we intend to the effect of migration of impurities on the step bunching induced by impurity.

[1] N. Cabrera and D. A. Vermilyea, in *Growth and Perpection of Crystals*, edited by R. Doremus, B. Roperts, and D. Turnbull (Wiley, New York, 1958), pp. 393–410.

[2] J. P. v. d. Eerden and H. Müller-Krumbhaar, Phys. Rev. Lett. **57**, 2431 (1986).

[3] D. Kandel and J. D. Weeks, Phys. Rev. Lett. **69**, 3758 (1992).

[4] D. Kandel and J. D. Weeks, Phys. Rev. B **49**, 5554 (1994).

[5] J. Krug, Europhys. Lett. **60**, 788 (2002).

[6] J. Vollmer, J. Hegedüs, F. Grosse, and J. Krug, New J. Phys. **10**, 053017 (2008).

[7] M. Ranganathan and J. D. Weeks, Phys. Rev. Lett. **110**, 055503 (2013).

[8] J. F. Ltsuko, N. Gonzáles-Segredo, M. A. Durán-Olivencia, A. E. S. Van Driessche, and M. Sleutel, Cryst. Growth Des. **14**, 6129 (2014).

[9] M. Ranganathan and J. D. Weeks, J. Cryst. Growth **393**, 35 (2014).

[10] M. Sleutel, J. F. Lutsko, D. Maes, and A. E. S. Van Driessche, Phys. Rev. Lett. **114**, 245501 (2015).

[11] J. F. Lutsko, A. E. S. Van Driessche, M. A. Durán-Olivencia, D. Maes, and M. Sleutel, Phys. Rev. Lett. **116**, 015501 (2016).

[12] M. Sleutel, J. Lutsko, and A. E. S. Van Driessche, Cryst. Growth Des. **18**, 171 (2018).

[13] A. Adawy, E. G. G. van der Heijden, J. Hekelaar, W. J. P. van Enckevort, W. J. De Grip, and E. Vlieg, Cryst. Growth Des. **15**, 1150 (2015).

[14] Y. Suzuki, K. Tsukamoto, I. Yoshizaki, H. Miura, and T. Fujiwara, Cryst. Growth Des. **15**, 4787 (2015).

[15] G. Dai, G. Sazaki, T. Matsui, K. Tsukamoto, K. Nakajima, Q. Kang, and W. Hu, Cryst. Growth Des. **11**, 88 (2011).

[16] M. Sato, Phys. Rev. E **84**, 061604 (2011).

[17] M. Sato, J. Phys. Soc. Jpn. **86**, 114603 (2017).

[18] A. E. S. Van Driesshe, G. Sazaki, G. Dai, F. Otálora, J. A. Gavira, T. Matsui, I. Yoshizaki, K. Tsukamoto, and K. Nakajima, Cryst. Growth Des. **9**, 3062 (2009).

[19] G. Ehrlich and F. G. Hudda, J. Chem. Phys. **44**, 1039 (1966).

[20] R. L. Schwoebel and E. J. Shipsey, J. Appl. Phys. **37**, 3682 (1966).

[21] Y. Saito and M. Uwaha, Phys. Rev. B **49**, 10677 (1994).

[22] Y. Saito, in *Statistical Physics of Crystal Growth* (World Scientific, Singapore, 1996).

[23] T. A. Land, T. L. Martin, S. Potapenko, G. T. Palmore, and J. J. De Yoreo, Nature (London) **399**, 442 (1999).